Am J Transl Res 2025;17(2):927-940
www.ajtr.org /ISSN:1943-8141/AJTR0162239

Original Article

Low-intensity ultrasound stimulation promotes differentiation of bone marrow mononuclear cells to nucleus pulposus cells for matrix synthesis

Chuang Li[1*], Yiqian He[1*], Ruosi Chen[2], Guangfu Miao[3], Jihao Cui[2]

[1]Department of Orthopedics, The Second Affiliated Hospital, Guangzhou Medical University, Guangzhou 510310, Guangdong, China; [2]Department of Spine Surgery, Hospital of Integrated Traditional Chinese and Western Medicine, Southern Medical University, Guangzhou 510310, Guangdong, China; [3]Department of Orthopedics and Traumatology, Hospital of Integrated Traditional Chinese and Western Medicine, Southern Medical University, Guangzhou 510310, Guangdong, China. [*]Equal contributors and co-first authors.

Received November 25, 2024; Accepted January 19, 2025; Epub February 15, 2025; Published February 28, 2025

Abstract: Objective: To investigate the role of low-intensity ultrasound stimulation (LIUS) in facilitating the differentiation of bone marrow mononuclear cells (BMMNCs) into nucleus pulposus cells (NPCs) for matrix synthesis, offering a possible new therapeutic approach for intervertebral disc degeneration. Methods: Human BMMNCs and NPCs were cultured, and exosomes were extracted from NPCs using differential ultracentrifugation, followed by characterization. LIUS was utilized to evaluate exosome uptake, induce cell differentiation, measure apoptosis, and track DNA synthesis by EdU assays. Various experimental conditions were tested, including different LIUS intensities and differentiation durations. A range of detection techniques, such as RT-qPCR, western blotting, and cellular staining, were employed to monitor relevant indicators. Results: Exosomes were successfully isolated from NPCs, and their purity was confirmed using nanoparticle tracking analysis (NTA), transmission electron microscopy, and western blot. PKH67-labeled exosomes were internalized by BMMNCs during co-incubation. LIUS treatment at different intensities revealed that the LIUS-100 group exhibited the most significant cell proliferation, as shown by EdU assays. Flow cytometry revealed that the LIUS-100 and LIUS-150 groups demonstrated the most pronounced inhibition of apoptosis. In NPC exosome-induced differentiation experiments, the expression of relevant marker mRNA and protein levels increased over time under standard conditions, with even greater upregulation observed under LIUS-100 stimulation. Moreover, LIUS-100 enhanced the intracellular accumulation of glycosaminoglycans and proteoglycans, suggesting its role in promoting BMMNC differentiation into NPCs and matrix component synthesis. Conclusion: NPC exosomes and LIUS are essential for guiding the differentiation of BMMNCs into NPCs, representing a promising therapeutic strategy for intervertebral disc degeneration. However, further *in vivo* studies are needed to refine LIUS technique, ensure safety, and evaluate long-term efficacy.

Keywords: Bone marrow mononuclear cells, nucleus pulposus cells, differentiation, low-intensity ultrasound stimulation

Introduction

Low back pain is among the most prevalent conditions worldwide, characterized by high clinical incidence, disability rate, and economic burden. It is also the leading non-cancerous disease associated with opioid prescriptions [1]. Over the coming decades, the disability and expenses attributed to low back pain are anticipated to rise significantly, particularly in developing countries where healthcare systems may be more vulnerable and less equipped to manage this escalating burden. Current clinical treatments for low back pain, whether conservative or surgical, primarily focus on symptom relief [2]. However, surgical intervention can disrupt the normal anatomy and biochemistry of the intervertebral discs, failing to address the primary cause of low back pain - intervertebral disc degeneration [3]. Given the limitations of existing treatments and the evolving understanding of the pathophysiologic mechanisms of intervertebral disc degeneration, such as cellular apoptosis, inflammation, and imbalances

https://doi.org/10.62347/LMPA6921

in matrix synthesis and metabolism, researchers have been exploring biotherapeutic strategies to repair or regenerate the degenerated intervertebral disc tissues [4]. Among these, cell therapy-based regenerative medicine stands out as a promising approach.

In healthy intervertebral discs, nucleus pulposus cells (NPCs) maintain a balance between the synthesis and degradation of the extracellular matrix (ECM) by secreting a variety of growth factors [5]. However, during intervertebral disc degeneration, NPCs lose their functionality, leading to alterations in the biochemical milieu. This includes a reduction in the expression of TGF-β, BMPs, and TIMPs, alongside increased expression of MMPs, TNF-α, IL-1β, IL-6, IL-8, prostaglandins, and nitric oxide [6]. These cytokine imbalances and inflammatory mediators further contribute to further deterioration of the microenvironment by inhibiting cellular functions, resulting in a drop in pH from the normal range of 7.0-7.2 to 6.8-6.2, increased hypoxia (oxygen levels falling to 1%, compared to the physiological range of 4-7%), reduced glucose and nutrient levels, and decreased osmotic pressure [7, 8]. The apoptosis and dysfunction of NPC, coupled with an adverse microenvironment, create a vicious cycle that accelerates intervertebral disc degeneration [9]. Clinically, this is characterized by discogenic low back pain, loss of disc height, and the decreased high signal intensity on T2-weighted MRI images. The reduction and dysfunction of NPC are recognized as key initiating factors in the degeneration process. Consequently, the implantation of exogenous cells with NPC functionality or potential to differentiate into NPCs represents a promising strategy for addressing intervertebral disc degeneration, potentially resolving the fundamental issues that underlie low back pain at a cellular level.

At present, the most widely investigated approach for cellular regeneration in intervertebral disc degeneration is cell therapy using mesenchymal stem cells (MSCs) [10, 11]. However, to enhance the therapeutic efficacy of MSCs in clinical setting, higher cell doses are often required. Yet, the injection of large cell volumes can lead to nutrient competition, which paradoxically results in the death of the implanted cells. Moreover, acquiring the large quantities of MSCs necessary for clinical application requires ex vivo expansion in Good Manufacturing Practice (GMP) - compliant facilities, which introduces costs and contamination risks, limiting the clinical translation of this approach. To address these limitations, recent attention has shifted towards bone marrow-derived mononuclear cells (BMMNCs). Prior research indicates that BMMNCs exhibit chondrogenic and osteogenic differentiation capabilities similar to those of MSCs expanded *ex vivo* [12]. Additionally, BMMNCs offer the benefits of rapid collection and transplantation procedures that can be performed within the operating room. The absence of a need for *ex vivo* cell culture in GMP facilities also reduces both costs and contamination risks. However, studies have shown that the harsh microenvironment of degenerated intervertebral discs, marked by hypoxia, decreased osmotic pressure, low glucose, high acidity, and abundant inflammatory mediators, significantly impairs the survival, phenotype, and function of injected cells [13]. There are also reports of cells dying rapidly post-implantation and becoming undetectable [14]. Consequently, we assume that BMMNCs may be unable to survive the destructive effects of the adverse microenvironment in degenerated intervertebral discs.

Low-intensity ultrasound stimulation (LIUS), a form of acoustic pressure wave that delivers localized mechanical stimulation to cells, has been approved by the FDA for clinical use in promoting bone fracture healing [15]. LIUS is thought to operate through the creation of a “deformation-induced microenvironment” along its path of propagation path, eliciting feedback effects at both genetic and cellular levels [16]. The oscillation of bubbles driven by LIUS alters microfluid dynamics and local shear stress, generating heat that subsequently affects cellular metabolism [17]. LIUS has been shown to significantly enhance the expression of chondrocyte-specific markers such as Col11II, Aggrecan, and COMP mRNA [18, 19]. Through interaction with integrins on chondrocytes and membrane-associated receptors, LIUS induces conformational changes in collagen, laminin, and fibronectin fibers, thereby activating both anabolic and catabolic intracellular pathways.

In this study, we investigated the effect of a six-channel ultrasound stimulation system employ-

ing low-intensity pulsed ultrasound on the differentiation of BMMNCs into NPCs *in vitro*.

Materials and methods

Cell culture

Human BMMNCs and NPCs, obtained from Saiye Biotechnology Co., Ltd., were cultivated in a complete medium consisting of DMEM/F-12 basal medium (Thermo Scientific, USA), supplemented with 10% fetal bovine serum (Sigma-Aldrich, USA) and 1% penicillin-streptomycin (Gibco, USA). The cells were maintained in an incubator set at 37°C with 5% CO_2 and 95% relative humidity. The culture medium was changed every three days, and cells were monitored under a microscope. When the cell confluence reached approximately 80%, the cells were sub-cultured at a 1:3 dilution ratio.

Isolation of NPC-derived exosomes

Exosomes from NPCs were isolated using a differential ultracentrifugation method. Once the NPCs reached 80% confluence in the third passage, the culture medium was replaced with serum-free DMEM/F-12 medium optimized for exosome collection. After a 48-hour incubation period, the supernatant was harvested and subjected to a series of centrifugation steps at 4°C to purify the exosomes. The first centrifugation was performed at 300 g for 10 minutes to pellet remaining cells, followed by a centrifugation at 2,000 g for 10 minutes to remove dead cells. A subsequent centrifugation at 10,000 g for 30 minutes eliminated cellular debris. The supernatant was then filtered through a 0.22 μm filter to clarify the solution and further centrifuged at 100,000 g for 70 minutes. The pellet was washed once with Phosphate-Buffered Saline (PBS, Thermo Scientific, USA), and the ultracentrifugation was repeated at 100,000 g for 70 minutes to ensure purity. The final pellet, containing the NPC-derived exosomes, was resuspended in 30-100 μl of PBS. Protein concentration was measured using the BCA assay, and the exosome samples were stored at -80°C for subsequent use.

Transmission electron microscopy analysis

The NPC-derived exosomes were diluted in PBS to a concentration of 200 μl/ml based on total protein content. 20 uL of this exosome suspension were then applied to a copper grid for sample preparation. After allowing the suspension to settle at room temperature for 1 minute, any excess liquid was gently absorbed with filter paper. Next, 10-30 μl of a 2% phosphotungstic acid solution (adjusted to pH 6.8) was added to the grid and incubated at room temperature for 1 minute to allow staining. The excess staining solution was carefully removed with filter paper, and the grid was air-dried under white light for 10 minutes. The morphology of the exosomes was subsequently examined and photographed using a transmission electron microscope.

Nanoparticle tracking analysis (NTA)

Cryopreserved exosome samples were thawed in a water bath at 25°C. After thawing, the samples were kept on ice during handling. The exosome samples were then diluted with PBS solution and used directly for NTA analysis. Detection and analysis were conducted using the ZetaVIEW S/N 17-310 nanoparticle tracking analyzer (PARTICLE METRIX GmbH).

Low-intensity ultrasound stimulation (LIUS)

The LIUS setup comprises a custom-designed function generator capable of handling six-channel outputs, coupled with 1 MHz ultrasound transducers, each with a diameter of 30 mm.

The LIUS parameters for our experiments were as follows: Frequency: 1 MHz; Pulse duration: 600 ms; Pulse repetition period: 3,000 ms; Pulse repetition frequency: 0.33 Hz; Duty cycle: 20%; Spatial-peak temporal-average intensity (ISPTA): 30-250 mW/cm^2.

Acoustic pressure was verified using a calibrated needle hydrophone (ONDA, Sunnyvale, CA, USA), with effective acoustic pressures in our experiments ranging from 0.05 to 0.14 MPa.

For *in vitro* cell stimulation studies, cells were initially cultured in six-well plates at a concentration of 2.5×10^4 cells/mL. Six transducers were positioned at the bottom of each well within the six-well plate to deliver 20-minute LIUS stimulation daily. A sham-treated control group was included, which underwent the same processing as the LIUS group, but without actual LIUS stimulation output.

Exosome uptake experiment

NPC-derived exosomes were labeled using the PKH67 fluorescent dye kit following the manufacturer's protocol (Sigma-Aldrich, USA). Under protected light conditions, 250 μg of NPC exosomes were resuspended in 1 mL of Solution C. Then, a 1×10^{-3} M stock solution of PKH67 was diluted to a working concentration of 2×10^{-6} M with 1 mL of Solution C. The NPC exosomes were thoroughly mixed with the PKH67 working solution, incubated for 5 minutes while protected from light. To neutralize any excess PKH67 dye, 2 mL of 5% BSA/PBS was added, and the mixture was centrifuged at 100,000 g for 70 minutes. The pellet was resuspended in 50 μL of PBS.

BMMNCs were prepared on slides. The PKH67-labeled NPC exosomes were introduced to the cell slides at a concentration of 50 ng/mL and incubated in the dark for different time points (0.5 h, 2 h, 4 h) to explore the relationship between exosome uptake and incubation duration.

At each time point, a control group was established with BMMNCs without the addition of NPC exosomes. At the end of the incubation period for each time point, the cell slides were retrieved, gently washed three times with PBS, fixed with pre-chilled 4% paraformaldehyde for 20 minutes, and washed again three times with PBS. The nuclei were stained with DAPI, and the slides were mounted on glass slides with glycerin for sealing. The cells were observed and imaged under a laser confocal microscope, and the images were analyzed using the LAS AF Lite software.

At 0.5 h, the PKH67-labeled NPC exosomes were taken up by BMMNCs to a limited extent, with only a few scattered punctate green fluorescence spots in the cytoplasm and no fluorescence on the cell membrane. After 2 h of incubation, the uptake increased but did not reach a stable state. At 4 h, the green fluorescence intensity and distribution within the cytoplasm of BMMNCs became stable, indicating that the exosome uptake had plateaued and met the requirements for subsequent experiments. Based on these observations, we determined 4 h as the appropriate exosome uptake time in our experiments.

Induction of BMMNCs to differentiate into nucleus pulposus-like cells by NPC exosomes

BMMNCs were seeded at a density of 2×10^5 cells per well in a 6-well culture plate. The cells were divided into four groups based on the differentiation induction duration: 3 days, 7 days, 11 days, and a control group of untreated BMMNCs. NPC exosomes were diluted in complete growth medium to a final concentration of 50 μg/ml, forming the exosome working solution. Each experimental group received 1.5 ml of the NPC exosome working solution. At the end of the designated induction periods, the stimulation was terminated, and the morphological changes in the BMMNCs were observed. The cells were then subjected to Alcian Blue and Type II Collagen immunohistochemical staining to assess the synthesis of glycosaminoglycans and Type II Collagen in the BMMNCs before and after induction. Concurrently, the expression levels of mRNA and proteins for nucleus pulposus markers were examined.

Cell apoptosis assay

Cells were plated at a density of 2.5×10^4 cells/mL in six-well culture plates and incubated for 24 to 48 hours to allow for attachment and growth. Following this, the cells were subjected to LIPUS stimulation for 20 minutes and then returned to the incubator for an additional 2 hours. The cells were harvested using trypsin to dissociate them into single cells. After being rinsed twice with PBS to remove remaining trypsin, the cells were resuspended in a binding buffer solution (500 μL) containing Annexin V-allophycocyanin (APC) (5 μL) and 7-aminoactinomycin D (7-AAD) (5 μL). This mixture was incubated for 10 minutes to allow the binding of the fluorescent probes to the cells, which were then analyzed for apoptosis using a flow cytometer.

EdU assay

The EdU incorporation assay was employed to quantify DNA synthesis, serving as an indicator of cell proliferation. The assay was conducted using the Click-iT EdU Imaging Kit (Thermo Fisher Scientific, Carlsbad, CA, USA) following the manufacturer's protocol as previously detailed. This method allowed for the precise measurement of cell proliferation rate under various experimental conditions.

RT-qPCR

RNA was carefully extracted using the ES-science RNA-Quick Purification Kit, ensuring high purity and integrity for downstream applications. Complementary DNA (cDNA) was synthesized from the purified RNA using the HiScript II Q RT SuperMix, optimized for qPCR. The expression levels of target RNA transcripts were quantified using SYBR Green on the Bio-Rad QX100 Droplet Digital PCR platform, a sensitive and reliable method for detecting and quantifying nucleic acids. Relative RNA expression levels were calculated using the $2^{-\Delta\Delta Ct}$ method, a widely used approach for normalizing gene expression data while accounting for variations in sample input and reverse transcription efficiency. The expression levels were normalized to the endogenous control gene glyceraldehyde 3-phosphate dehydrogenase (GAPDH), which served as a reference to ensure the accuracy and consistency of the results across different samples and experimental conditions.

Western blotting

Protein extraction from cells was performed using cold RIPA buffer (Beyotime), supplemented with protease and phosphatase inhibitors (Thermo Scientific, USA) to prevent degradation. Protein concentrations were measured using the BCA Protein Assay Kit (Thermo Scientific, USA).

For western blotting, equal amounts of protein samples (20-30 μg per lane, depending on the protein abundance and the resolution required) were separated by 4-12% SDS-PAGE and transferred onto 0.45 μm PVDF membranes (Millipore, USA).

The membranes were blocked with 5% skim milk in TBST for 60 minutes at room temperature to reduce non-specific binding. Subsequently, the membranes were incubated with primary antibodies overnight at 4°C. The primary antibodies used, and their dilutions were as follows: Anti-Aggrecan antibody (ab313636, Abcam, UK), 1:1,000; Anti-Collagen II antibody (ab34712, Abcam, UK), 1:2,000; Anti-Sox-9 antibody (ab185966, Abcam, UK), 1:2,500; Anti-KRT19 antibody (ab52625, Abcam, UK), 1:50,000; Anti-β-actin antibody (ab5694, Abcam, UK), 1:1,000 (loading control).

After incubation with primary antibodies, the membranes were washed three times with TBST for 10 minutes each to remove unbound primary antibodies. Then, the membranes were incubated with HRP-conjugated secondary antibodies (ab150077, Abcam, UK) diluted 1:1,000, for 60 minutes at room temperature.

Finally, bands were detected using a Bio-Rad imaging system with an ECL detection kit (Servicebio, Wuhan, China). Band intensity was quantified using ImageJ software, and the relative expression levels of the target proteins were calculated relative to the loading control (β-actin).

Proteoglycan and glycosaminoglycan staining

BMMNCs were seeded at a density of 2×10^5 cells per well in a 6-well plate and were subjected to the treatment groups as previously described. On the seventh day, the cell culture medium was removed, and the cells were rinsed twice with PBS solution. Following this, 1 mL of 4% paraformaldehyde fixative was added for a 30-minute fixation period. After the fixative was discarded, the cells were rinsed twice with PBS solution again. For staining, 1 mL of Safranin O staining solution was applied for 30 minutes to visualize proteoglycans, or 1 mL of Alcian Blue staining solution was used for a 1-hour incubation to stain glycosaminoglycans. The cells were then examined using an inverted microscope to observe and document the staining of the extracellular matrix components.

Statistical analysis

Statistical analyses were conducted using GraphPad Prism software (version 7.0), employing one-way or two-way analysis of variance (ANOVA) as appropriate. All experiments were conducted in triplicate to ensure reproducibility and robustness of the findings. The results were presented as mean ± standard deviation. Significance levels were set at *P<0.05, **P< 0.01, and ***P<0.001.

Results

Isolation and identification of exosomes from NPC

Exosomes secreted by NPCs were purified using differential ultracentrifugation. NTA anal-

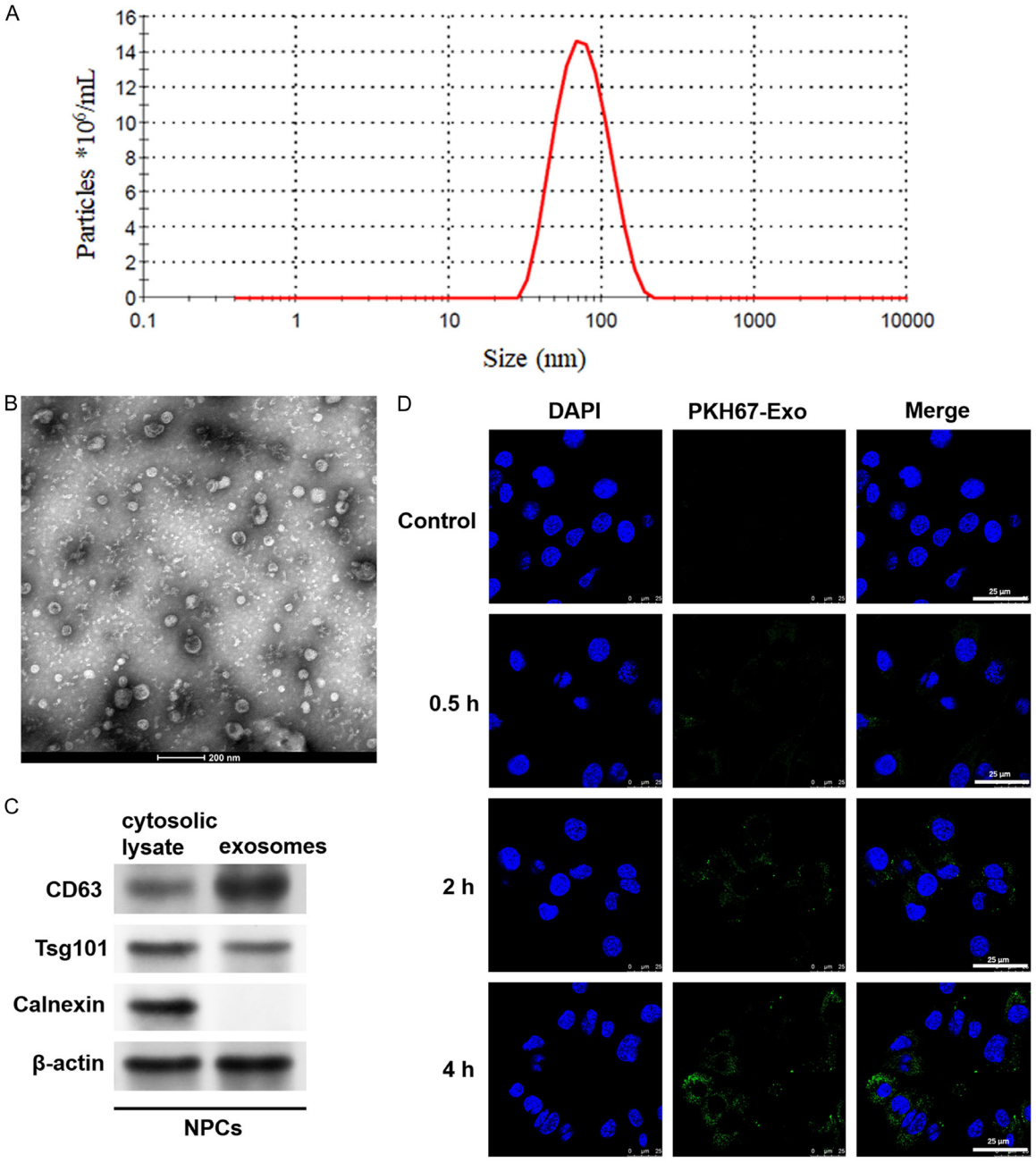

Figure 1. Isolation and identification of exosomes from NPCs. A: After isolating and purifying NPC exosomes using differential ultracentrifugation, their size distribution was analyzed with NTA. B: The dimensions and morphology of the harvested NPC exosomes were examined using transmission electron microscopy. C: The presence of exosomal marker proteins CD63 and Tsg101, along with the endoplasmic reticulum marker Calnexin, was assessed by western-blot analysis. D: Exosomes were labeled with the lipophilic fluorescent dye PKH67 and then co-incubated with BMMNCs. The subsequent uptake of NPC exosomes by these cells was visualized under a laser confocal microscope. Magnification: ×400. Data: Mean ± SEM. n=3. BMMNCs, bone marrow mononuclear cells; NPCs, nucleus pulposus cells.

ysis confirmed that the exosome size were between 50 nm and 150 nm (**Figure 1A**). The extracted vesicles from the NPC matrix, stained with phosphotungstic acid and viewed under an electron microscope at magnifications of 80,000-120,000 times, exhibited round or oval shapes with distinct boundaries, aligning with the characteristics of standard exosomes

(**Figure 1B**). Western-blot analysis (**Figure 1C**) indicated high expression levels of exosomal marker proteins CD63 and Tsg101 in the NPC exosomes. Notably, there was an absence of Calnexin, a marker for the endoplasmic reticulum typically associated with cell debris from lysis, was absent, confirming the purity of NPC exosomes with minimal contamination from disrupted cellular organelles. Moreover, following a 4-hour incubation of PKH67-labeled NPC exosomes with BMMNCs, confocal microscope showed dispersed punctate green fluorescence within the cytoplasm of BMMNCs, but no fluorescence on the cell membrane, indicating internalization of NPC exosomes by BMMNCs, likely through phagocytosis (**Figure 1D**).

LIUS enhanced BMMNC proliferation and inhibited apoptosis

In subsequent experiments, we applied LIUS at varying intensities using a six-channel ultrasound stimulation system to BMMNCs. The intensities, expressed as spatial peak temporal average (ISPTA), were set at 0, 30, 50, 70, 100, 150, 200, and 250 mW/cm^2. EdU assays were then conducted to evaluate the proliferative response of BMMNCs to these LIUS intensities, revealing that the LIUS-100 group exhibited the highest proliferation rate (**Figure 2A**). Additionally, flow cytometry analysis revealed that the LIUS-100 and LIUS-150 groups exhibited the most significant inhibition of apoptosis (**Figure 2B**). Consequently, we selected LIUS-100 as the optimal intensity for further investigation.

LIUS stimulation enhanced the differentiation of BMMNCs into NPCs induced by NPC exosomes

BMMNCs were treated with exosomes derived from NPCs under either standard culture conditions or with LIUS-100 stimulation for durations of 3, 7, and 14 days to induce their differentiation into NPCs. RT-qPCR analysis was employed to assess the transcriptional and protein expression of NPC differentiation markers and extracellular matrix synthesis markers in BMMNCs, including Aggrecan, Collagen II, Sox-9, and KRT19. The findings indicated that, with NPC exosome treatment under standard culture conditions, the mRNA and protein levels of Aggrecan, Collagen II, Sox-9, and KRT19 in BMMNCs were significantly upregulated over time (**Figures 3**, **4**), demonstrating that the NPC exosomes can drive the differentiation of BMMNCs into NPCs. Strikingly, under LIUS-100 stimulation, the upregulation of Aggrecan, Collagen II, Sox-9, and KRT19 was even more pronounced, suggesting that LIUS-100 stimulation can expedite the differentiation process of BMMNCs into NPC facilitated by NPC exosomes.

LIUS stimulation enhanced the accumulation of glycosaminoglycans and proteoglycans induced by NPC exosomes in BMMNCs

Following a 7-day induction period, BMMNCs were stained for intracellular glycosaminoglycans and proteoglycans using Alcian Blue and Safranin O. The findings demonstrated that under standard culture conditions, treatment with NPC exosomes resulted in an increased staining intensity for both glycosaminoglycans and proteoglycans within BMMNCs (**Figure 5A**). This enhancement was further amplified under LIUS-100 stimulation (**Figure 5B**), suggesting that LIUS-100 stimulation indeed accelerates the differentiation of BMMNCs into NPCs induced by NPC exosomes.

The elevated staining intensity observed under both conditions reflects a greater accumulation of glycosaminoglycans and proteoglycans, which are essential components of the extracellular matrix and play key roles in cellular signaling and tissue hydration. The pronounced enhancement under LIUS-100 stimulation indicates that the mechanical effects of ultrasound may foster a more conducive microenvironment for differentiation. This observation highlights the benefit of combining LIUS with NPC exosome treatment as a strategy to augment the regenerative potential of BMMNCs in therapeutic contexts.

Discussion

Intervertebral disc degeneration-induced back pain presents a substantial global health challenge. Existing treatment approaches often focus on alleviating symptoms rather than tackling the underlying degenerative processes. Cell-based therapies, including those utilizing MSCs and BMMNCs, have shown promising potential but also encounter significant hurdles. MSCs necessitate extensive cell numbers and ex vivo expansion, raising concerns about

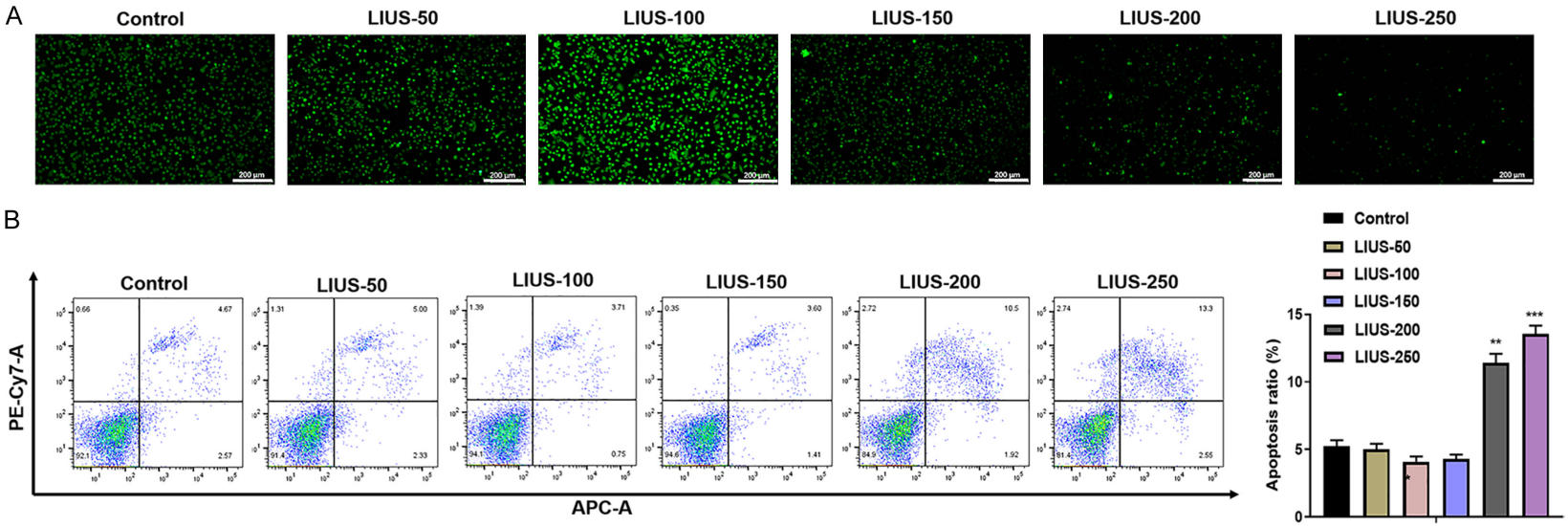

Figure 2. LIUS enhanced BMMNC proliferation and inhibited apoptosis. A: The proliferation of BMMNCs was assessed using EdU assays following exposure to a range of ISPTA levels (0, 30, 50, 70, 100, 150, 200, and 250 mW/cm^2). Magnification: ×50. B: Flow cytometry analysis was conducted to evaluate the apoptotic response of BMMNCs to the same spectrum of ISPTA levels (0, 30, 50, 70, 100, 150, 200, and 250 mW/cm^2). Data: Mean ± SEM. n=3. $^{**}P<0.01$, $^{***}P<0.001$ vs Control group. BMMNCs, bone marrow mononuclear cells; NPCs, nucleus pulposus cells.

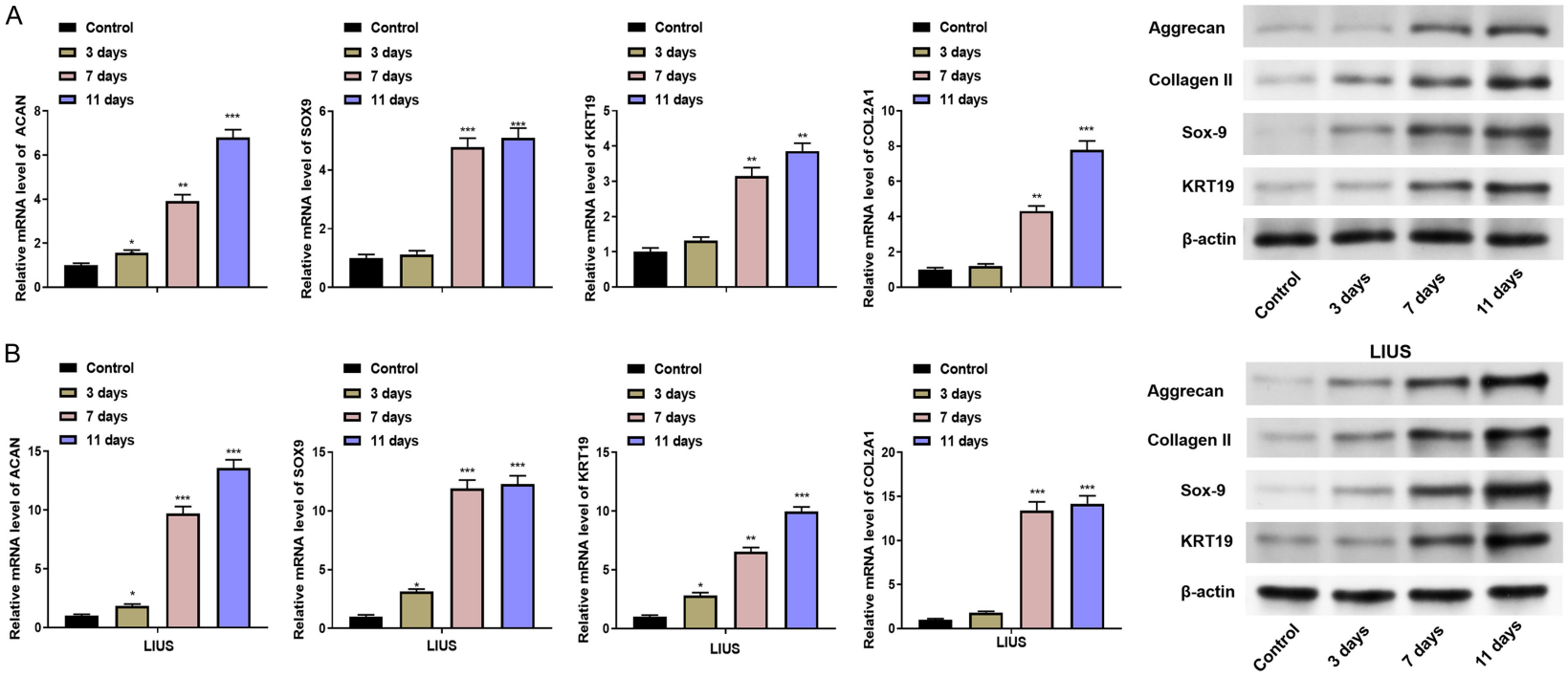

Figure 3. LIUS stimulation enhanced the differentiation of BMMNCs into NPCs induced by NPC exosomes. A: RT-qPCR analysis was conducted to evaluate the transcriptional levels of markers indicative of NPC differentiation and extracellular matrix synthesis in BMMNCs, encompassing Aggrecan, Collagen II, Sox-9, and KRT19. B: RT-qPCR analysis was performed to determine the mRNA levels of these NPC differentiation and extracellular matrix synthesis markers in BMMNCs, which included Aggrecan, Collagen II, Sox-9, and KRT19, exposure to LIUS. Data: Mean ± SEM. n=3. **P*<0.05, ***P*<0.01, ****P*<0.001 vs Control group. BMMNCs, bone marrow mononuclear cells; NPCs, nucleus pulposus cells.

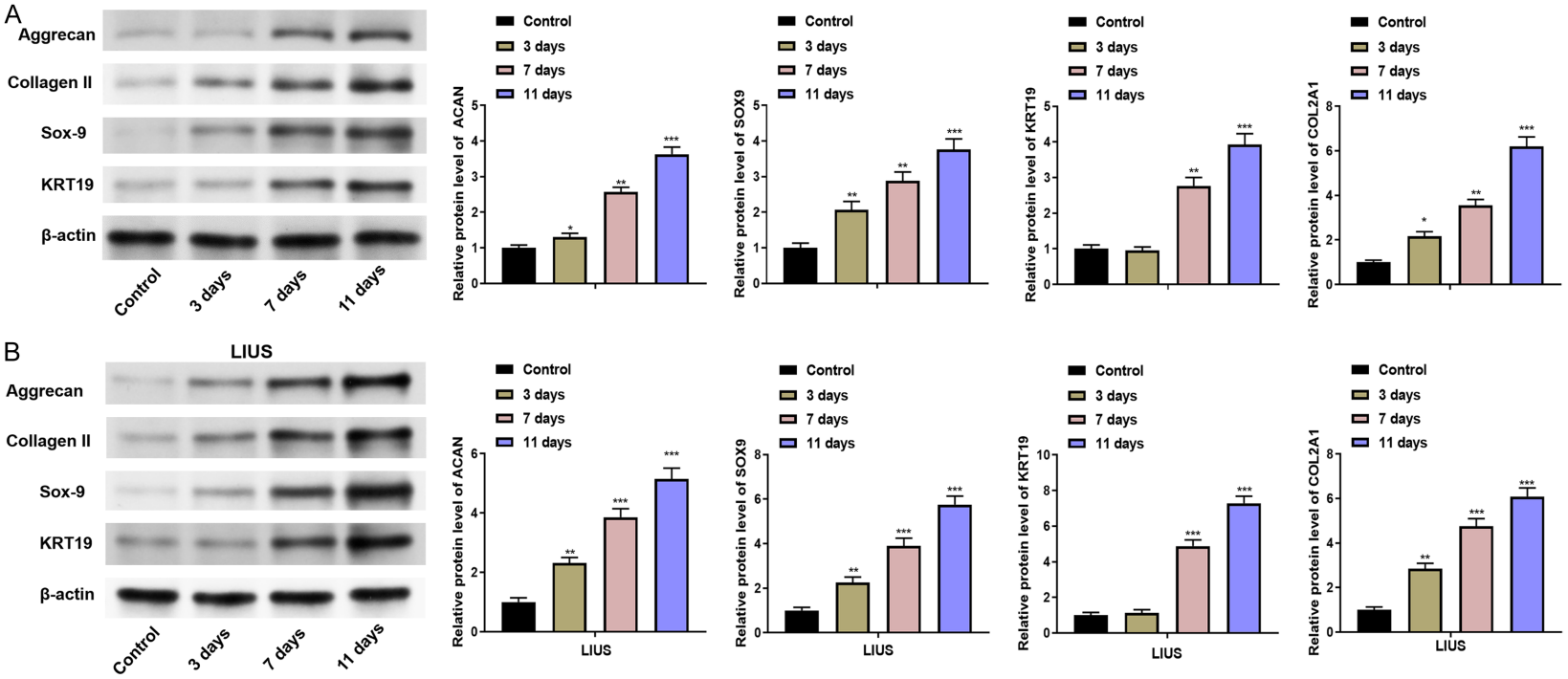

Figure 4. LIUS stimulation enhanced the differentiation of BMMNCs into NPCs induced by NPC exosomes. A: Western blotting analysis was conducted to evaluate the protein levels of markers indicative of NPC differentiation and extracellular matrix synthesis in BMMNCs, encompassing Aggrecan, Collagen II, Sox-9, and KRT19. B: Western blotting analysis was performed to determine the protein levels of these NPC differentiation and extracellular matrix synthesis markers in BMMNCs, which included Aggrecan, Collagen II, Sox-9, and KRT19, exposure to LIUS. Data: Mean ± SEM. n=3. **P*<0.05, ***P*<0.01, ****P*<0.001 vs. Control group. BMMNCs, bone marrow mononuclear cells; NPCs, nucleus pulposus cells.

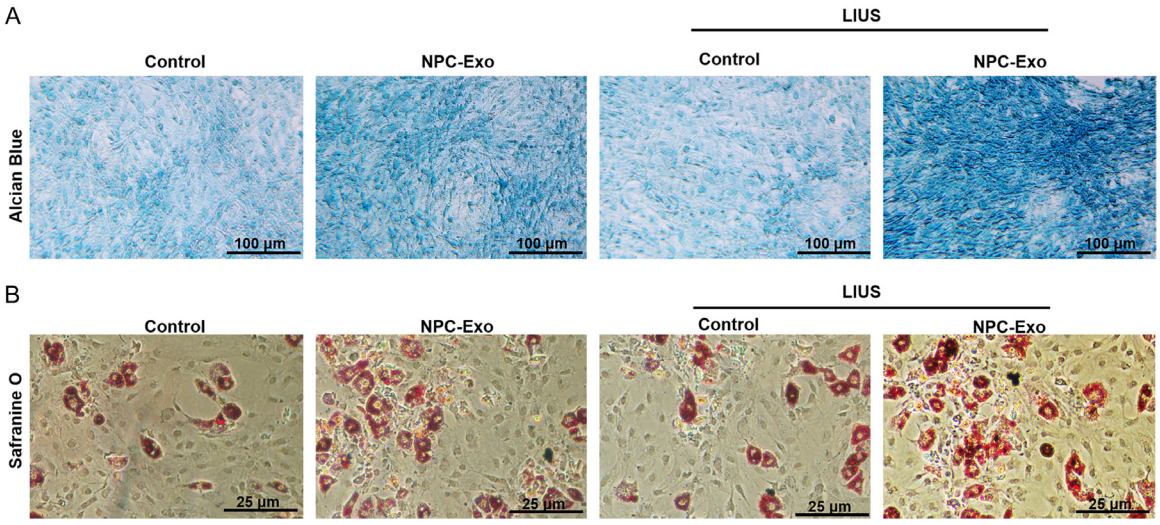

Figure 5. LIUS stimulation enhanced the accumulation of glycosaminoglycans and proteoglycans induced by NPC exosomes in BMMNCs. A: Glycosaminoglycans in bone marrow mononuclear cells across all groups were stained using Alcian Blue. Magnification: ×100. B: Proteoglycans in bone marrow mononuclear cells across all groups were stained using Safranin O. Magnification: ×400. Data: Mean ± SEM. n=3. BMMNCs, bone marrow mononuclear cells; NPCs, nucleus pulposus cells.

cost and contamination risks. On the other hand, while BMMNCs can be collected and transplanted more rapidly, their survival and efficacy within the hostile microenvironment of degenerated discs are often limited. Our research endeavors to surmount these limitations by investigating an innovative method that integrates the biological effects of NPC exosomes with the mechanical stimulation provided by LIUS.

NPC exosomes played a central role in our investigation. Their isolation and characterization were meticulously conducted to confirm their purity and functionality. These exosomes were confirmed to fall within the expected size range of 50-150 nm, presenting with the characteristic round or oval morphology and well-defined edges. Western-blot analysis affirmed the presence of canonical exosomal marker proteins, CD63 and Tsg101, while the absence of Calnexin suggested minimal contamination from cellular organelles. Upon co-incubation with BMMNCs, the NPC exosomes were internalized, presumably via phagocytosis, enabling the transfer of biomolecular messages from the exosomes to the target cells. Rich in growth factors, cytokines, and miRNAs, NPC exosomes can modulate the behavior of recipient cells. In our study, NPC exosomes were demonstrated to stimulate the differentiation of BMMNCs into NPCs under standard culture conditions. The progressive upregulation of mRNA and protein levels for NPC differentiation markers such as Aggrecan, Collagen II, Sox-9, and KRT19 over time underscored the potency of exosomes in driving cellular differentiation. This aligns with existing literature on the role of exosomes in cellular communication and tissue regeneration.

BMMNCs, found in the bone marrow, are immature mononuclear cells considered as precursors to osteoclasts. Isolated from bone marrow aspirates by density gradient centrifugation, these cells exhibit stem cell-like characteristics [20, 21]. After completing their final mitotic phase, BMMNCs remain in the bone marrow for about 38 hours before swiftly entering the circulation to replenish lost cells. During differentiation, BMMNCs can give rise to various bone cell types, encompassing osteoblasts, chondrocytes, and osteoclasts [12, 22, 23]. Studies have indicated that specific inducers like macrophage colony-stimulating factor and nuclear factor κB receptor activator ligand, can foster the differentiation of BMMNCs into osteoclasts *in vitro* [24]. Moreover, single-cell transcriptome sequencing has unveiled the heterogeneity and differentiation potential of NPCs. For example, CD90-positive nucleus pulposus cells exhibit robust growth and differentiation capa-

bilities, giving rise to various cellular lineages, including osteoblasts and adipocytes [25]. These insights offer novel insights into the differentiation mechanisms of nucleus pulposus cells and broaden the horizon for applications in regenerative medicine and tissue engineering.

LIUS significantly affected BMMNCs in this study. The application of LIUS at varying intensities demonstrated that the LIUS-100 group exhibited the most robust proliferation, as determined by EdU assays. This suggests that a specific LIUS intensity can effectively stimulate BMMNC growth. Additionally, flow cytometry analysis revealed that both the LIUS-100 and LIUS-150 groups showed the greatest inhibition of apoptosis, highlighting LIUS's potential to improve cell survival and functionality *in vivo*. The influence of LIUS on the differentiation of BMMNCs into NPCs primarily operates through the activation of intracellular signaling pathways, which promote both cell proliferation, differentiation, and extracellular matrix formation. Kobayashi *et al*. [26] found that LIUS could upregulate the expression of several matrix-related genes, including those associated with growth factors, thereby enhancing the proliferation of human nucleus pulposus cells and the production of proteoglycans. Furthermore, low-intensity ultrasound can stimulate intracellular calcium ion fluctuations, aiding osteoblast differentiation [27]. These findings indicate that LIUS not only promotes BMMNC differentiation into NPCs, potentially by regulating intracellular signaling pathways and calcium ion concentrations. Consequently, LIPUS, as an emerging and effective adjuvant therapy, holds significant promise for skeletal repair and regeneration. Its effects may involve the creation of a "deformation-induced microenvironment", where the oscillation of bubbles driven by LIUS alters microfluid dynamics and local shear stress, influencing cellular metabolism. This intricate mechanism may also interact with the biological effects of NPC exosomes, further enhancing the differentiation of BMMNCs into NPCs.

The combination of LIUS and NPC exosomes showed a synergistic effect on the differentiation of BMMNCs into NPCs. Under LIUS-100 stimulation, the enhancement of mRNA and protein levels for Aggrecan, Collagen II, Sox-9, and KRT19 was even more pronounced compared to treatment with NPC exosomes alone. This suggests that LIUS can enhance the biological effects of the exosomes, possiblyby optimizing the microenvironment for cell differentiation. Additionally, the enhanced accumulation of glycosaminoglycans and proteoglycans under LIUS-100 stimulation further supports this synergistic effect. These molecules are important components of the extracellular matrix, and their increased accumulation indicates a more favorable environment for cell differentiation and tissue regeneration. The mechanical effects of LIUS may work in concert with the biological signals carried by the exosomes to promote the differentiation process. This combination approach may offer a more effective strategy for treating intervertebral disc degeneration compared to using either LIUS or NPC exosomes alone. Furthermore, our experimental data suggest that LIUS stimulation likely influences the interaction between NPC-exosomes and BMMNCs, affecting the intracellular accumulation of glycosaminoglycans and proteoglycans. This effect may stem from LIUS's ability to modify the cellular microenvironment, potentially through mechanical vibrations and thermal effects, which could influence exosome uptake, release, and the activity of their biomolecules. In the presence of NPC-exosomes, LIUS may enhance exosome-cell binding and expedite the internalization of exosomal biomolecules, thereby impacting cellular metabolic processes and leading to increased accumulation of glycosaminoglycans and proteoglycans. In contrast, in control cell groups lacking NPC-exosomes, LIUS might not exert its effects through the same mechanisms. These findings underscore the critical and unique role of LIUS in facilitating BMMNC differentiation when combined with NPC-exosomes, shedding light on the potential of this combined approach for tissue regeneration.

The findings of this study have several implications for clinical application. First, the ability of LIUS to enhance the survival and functionality of BMMNCs in vitro suggests that it may have similar beneficial effect *in vivo*, potentially improving the outcomes of cell-based therapies for intervertebral disc degeneration. Second, the combination of LIUS and NPC exosomes may offer a more effective treatment option compared to current cell-based thera-

pies. By optimizing the microenvironment for cell differentiation and enhancing the biological effects of the exosomes, this approach may address some of the limitations associated with MSCs and BMMNCs. However, several challenges need to be addressed before clinical translation. The *in vitro* results need to be validated in appropriate animal models. Additionally, the optimal parameters for LIUS application, such as intensity, frequency, and duration of stimulation, require further investigation. Additionally, the safety and long-term efficacy of this combination approach need to be further evaluated. Despite these challenges, the results of this study provide a promising foundation for future research in the field of intervertebral disc degeneration treatment.

Future research should focus on several aspects to further develop this approach. First, *in vivo* studies using animal models are essential to validate the *in vitro* findings. These studies should investigate the effects of LIUS and NPC exosomes on intervertebral disc degeneration, including changes in disc height, pain relief, and histological improvements. Second, a more precise determination of the optimal parameters for LIUS application is needed. This may involve exploring varying intensities, frequencies, and durations of stimulation to identify the most effective combination. Third, the mechanisms underlying the synergistic effects of LIUS and NPC exosomes need to be further elucidated. Understanding these mechanisms will help to optimize the treatment approach and develop more targeted therapies. In addition, research should also explore the potential of other cell sources and exosomes in combination with LIUS for intervertebral disc degeneration treatment. Different cell types may offer unique properties that could lead to better treatment outcome. The development of more efficient exosome isolation and purification could enhance the quality and reproducibility of the treatment. Finally, the long-term safety and efficacy of this combination approach need to be continuously monitored and evaluated to ensure its suitability for clinical application.

In conclusion, this study has provided valuable insight into the possibility of combining LIUS and NPC exosomes for the treatment of intervertebral disc degeneration. The results suggest a synergistic effect that can enhance the differentiation of BMMNCs into NPC and improve the regenerative potential of these cells. While there are still challenges to be addressed before clinical translation, this study paves the way for future research in this exciting field.

Acknowledgements

This work is supported by Guangdong Basic and Applied Basic Research Foundation (No. 2021A1515012190).

Disclosure of conflict of interest

None.

Address correspondence to: Jihao Cui, Department of Spine Surgery, Hospital of Integrated Traditional Chinese and Western Medicine, Southern Medical University, No. 13 Shiliugang Road, Haizhu District, Guangzhou 510310, Guangdong, China. E-mail: cuijh020@163.com

References

[1] Farley T, Stokke J, Goyal K and DeMicco R. Chronic low back pain: history, symptoms, pain mechanisms, and treatment. Life (Basel) 2024; 14: 812.

[2] Evans L, O'Donohoe T, Morokoff A and Drummond K. The role of spinal surgery in the treatment of low back pain. Med J Aust 2023; 218: 40-45.

[3] Chiu AP, Chia C, Arendt-Nielsen L and Curatolo M. Lumbar intervertebral disc degeneration in low back pain. Minerva Anestesiol 2024; 90: 330-338.

[4] Diwan AD and Melrose J. Intervertebral disc degeneration and how it leads to low back pain. JOR Spine 2022; 6: e1231.

[5] Li YX, Ma XX, Zhao CL, Wei JH, Mei AH and Liu Y. Nucleus pulposus cells degeneration model: a necessary way to study intervertebral disc degeneration. Folia Morphol (Warsz) 2023; 82: 745-757.

[6] Tan Z, Chen P, Dong X, Guo S, Leung VYL, Cheung JPY, Chan D, Richardson SM, Hoyland JA, To MKT and Cheah KSE. Progenitor-like cells contributing to cellular heterogeneity in the nucleus pulposus are lost in intervertebral disc degeneration. Cell Rep 2024; 43: 114342.

[7] Zhang X, Lv Z and Wei C. Hypo-osmolality activates Wnt/β-catenin mediated by AQP1 in nucleus pulposus cells degeneration. Cell Mol Biol (Noisy-le-grand) 2024; 70: 194-199.

[8] Chu G, Zhang W, Han F, Li K, Liu C, Wei Q, Wang H, Liu Y, Han F and Li B. The role of mi-

croenvironment in stem cell-based regeneration of intervertebral disc. Front Bioeng Biotechnol 2022; 10: 968862.
[9] Zhou D, Mei Y, Song C, Cheng K, Cai W, Guo D, Gao S, Lv J, Liu T, Zhou Y, Wang L, Liu B and Liu Z. Exploration of the mode of death and potential death mechanisms of nucleus pulposus cells. Eur J Clin Invest 2024; 54: e14226.
[10] Zhang QX and Cui M. How to enhance the ability of mesenchymal stem cells to alleviate intervertebral disc degeneration. World J Stem Cells 2023; 15: 989-998.
[11] Baldia M, Mani S, Walter N, Kumar S, Srivastava A and Prabhu K. Bone marrow-derived mesenchymal stem cells augment regeneration of intervertebral disc in a reproducible and validated mouse intervertebral disc degeneration model. Neurol India 2021; 69: 1565-1570.
[12] Peeters JAHM, Peters HAB, Videler AJ, Hamming JF, Schepers A and Quax PHA. Exploring the effects of human bone marrow-derived mononuclear cells on angiogenesis in vitro. Int J Mol Sci 2023; 24: 13822.
[13] Clouet J, Fusellier M, Camus A, Le Visage C and Guicheux J. Intervertebral disc regeneration: from cell therapy to the development of novel bioinspired endogenous repair strategies. Adv Drug Deliv Rev 2019; 146: 306-324.
[14] Acosta FL Jr, Metz L, Adkisson HD, Liu J, Carruthers-Liebenberg E, Milliman C, Maloney M and Lotz JC. Porcine intervertebral disc repair using allogeneic juvenile articular chondrocytes or mesenchymal stem cells. Tissue Eng Part A 2011; 17: 3045-3055.
[15] Qin PP, Jin M, Xia AW, Li AS, Lin TT, Liu Y, Kan RL, Zhang BB and Kranz GS. The effectiveness and safety of low-intensity transcranial ultrasound stimulation: a systematic review of human and animal studies. Neurosci Biobehav Rev 2024; 156: 105501.
[16] Du M, Li Y, Zhang Q, Zhang J, Ouyang S and Chen Z. The impact of low intensity ultrasound on cells: underlying mechanisms and current status. Prog Biophys Mol Biol 2022; 174: 41-49.
[17] Song H, Chen R, Ren L, Zeng Y, Sun J and Tong S. Low intensity transcranial ultrasound stimulation induces hemodynamic responses through neurovascular coupling. iScience 2024; 27: 110269.
[18] Sabanci S, Sabanci S, Sendur OF, Sakarya S and Yilmaz O. The effectiveness of therapeu tic ultrasound to the mechanically damaged chondrocyte culture. Physiother Theory Pract 2024; 40: 21-30.
[19] Jo NG, Ko MH, Won YH, Park SH, Seo JH and Kim GW. The efficacy of low-intensity pulsed ultrasound on articular cartilage and clinical evaluations in patients with knee osteoarthritis. J Back Musculoskelet Rehabil 2022; 35: 1381-1389.
[20] Nguyen QT, Thanh LN, Hoang VT, Phan TTK, Heke M and Hoang DM. Bone marrow-derived mononuclear cells in the treatment of neurological diseases: knowns and unknowns. Cell Mol Neurobiol 2023; 43: 3211-3250.
[21] Eweida A, Flechtenmacher S, Sandberg E, Schulte M, Schmidt VJ, Kneser U and Harhaus L. Systemically injected bone marrow mononuclear cells specifically home to axially vascularized tissue engineering constructs. PLoS One 2022; 17: e0272697.
[22] Lee SA, Kim S, Kim SY, Park JY, Nan J, Park HS, Lee H, Lee YD, Lee H, Kang S, Jung HS, Chung SS and Park KS. Direct differentiation of bone marrow mononucleated cells into insulin-producing cells using 4 specific soluble factors. Stem Cells Transl Med 2023; 12: 485-495.
[23] Mendoza R, Banerjee I, Manna D, Reghupaty SC, Yetirajam R and Sarkar D. Mouse bone marrow cell isolation and macrophage differentiation. Methods Mol Biol 2022; 2455: 85-91.
[24] Kylmäoja E, Nakamura M, Turunen S, Patlaka C, Andersson G, Lehenkari P and Tuukkanen J. Peripheral blood monocytes show increased osteoclast differentiation potential compared to bone marrow monocytes. Heliyon 2018; 4: e00780.
[25] Han S, Zhang Y, Zhang X, Zhang H, Meng S, Kong M, Liu X and Ma X. Single-cell RNA sequencing of the nucleus pulposus reveals chondrocyte differentiation and regulation in intervertebral disc degeneration. Front Cell Dev Biol 2022; 10: 824771.
[26] Kobayashi Y, Sakai D, Iwashina T, Iwabuchi S and Mochida J. Low-intensity pulsed ultrasound stimulates cell proliferation, proteoglycan synthesis and expression of growth factor-related genes in human nucleus pulposus cell line. Eur Cell Mater 2009; 17: 15-22.
[27] Maung WM, Nakata H, Miura M, Miyasaka M, Kim YK, Kasugai S and Kuroda S. Low-intensity pulsed ultrasound stimulates osteogenic differentiation of periosteal cells in vitro. Tissue Eng Part A 2021; 27: 63-73.